Intrinsic freedom of dislocation structures and Peierls stress oscillation

Shaofeng Wang*

Institute for Structure and Function and Department of Physics, Chongqing University, Chongqing 401331, People's Republic of China

(Received 6 October 2021; revised 6 March 2022; accepted 8 March 2022; published 25 March 2022)

When the continuous translation symmetry breaks, a continuous mode splits into two distinct discrete modes with different energies. Based on the fully discrete Peierls model, it is found that stability of such discrete modes for dislocations can be tuned by the stacking fault energy of a slip system. As the stacking fault energy changes continuously, the stable dislocation structure transforms periodically and the Peierls stress varies oscillatorily. Furthermore, at the transformation point, the lattice resistance nearly vanishes and thus the dislocation can almost move freely.

DOI: 10.1103/PhysRevB.105.094113

I. INTRODUCTION

The dislocation is a kind of structural defect of solids [1] and it can be viewed as a nonlinear mode protected by topology. In the elastic continuum theory of solids, an individual dislocation is a singular line carrying topology charge characterized by the Burgers vector. However, even with a minimum lattice vector as the Burgers vector, a dislocation possesses extended structures instead of being line singularity. Because dislocation properties are mainly determined by structure, a great effort has been made in understanding the dislocation structure [2–16].

The most successful theory of dislocation structure is the Peierls-Nabarro (PN) model that can predict the core width and the Peierls stress analytically [2]. In particular, with the aid of the generalized stacking fault energy (γ surface), which can be calculated directly from the electron density functional theory, the PN model has been widely used to investigate dislocations in a variety of materials [7,9,10,12,14,15]. In the classical PN model, dislocation structures are dominated by a nonlinear integrodifferential equation, and thus the lattice discreteness is not considered sufficiently.

When the lattice discreteness breaks continuous translation symmetry in the continuum theory, the continuous mode splits into two types of symmetrically discrete modes. As illustrated in Fig. 1, the first type has its symmetry center just on the lattice point and can be properly referred to as the O mode. The second type has its symmetry center between two neighboring lattice points and can be properly referred to as the B mode. Although both the B mode and the O mode are equilibrium configurations, their energies are different. The mode with the lower energy is stable. The existence of two different discrete modes naturally leads to an important question: which mode is stable? The stable mode is observable in experiments. If one type mode always has the lower energy, this type of mode will be observed in experiments and the other type of mode will never exist stationarily because the high energy mode is unstable. If the mode stability is not fixed, one mode may be stable in some materials and the other mode may be stable in other materials. It is therefore necessary to recognize exactly which type of mode is stable. In particular, if the mode stability can be changed, both the B mode and the O mode must be considered on an equal basis. In this paper, it is shown that the stability of the B mode and the O mode for the dislocation can be tuned by the stacking fault energy. As the stacking fault energy changes, the mode stability exchanges periodically. The transformation between the B mode and the O mode implies that there is structural freedom beyond the continuous density distribution given in the classical PN theory. Furthermore, it is found that, at the transformation point, the lattice resistance nearly vanishes and the dislocation almost moves freely. As a consequence, material plasticity dominated by dislocation mobility should undergo substantial change when passing the transition point. These theoretical results suggest a possible way for modifying and controlling material mechanical properties by using this freedom of dislocation structure.

II. SPECTRUM MODEL

Appearance of a straight dislocation is the result of a nonuniformly relative slip between two neighboring lattice planes (slip planes). The energy related to the relative slip consists of the elastic energy stored in crystal body and the misfit energy resulting from the mismatch of the gliding planes. Within the harmonic approximation of the interaction among the atoms in a solid, the elastic energy can be generally written as

$$U_e = \frac{1}{2}\sum_{l=-\infty}^{\infty}\sum_{l'=-\infty}^{\infty}\Omega(l-l')S(l)S(l'), \tag{1}$$

where integers l and l' are used to label the parallel atom chains on a slip plane, $S(l)$ is the slip field defined by the local relative displacement between the two slip planes, and $\Omega(l)$ is the discrete kernel describing effective interaction of the slip field. The discrete kernel $\Omega(l)$ can be formally obtained

*sfwang@cqu.edu.cn

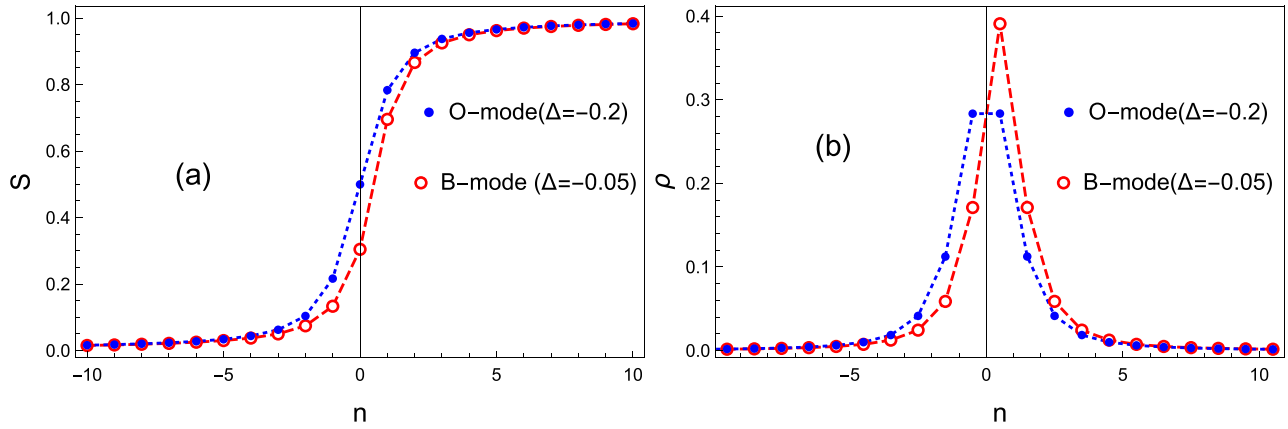

FIG. 1. B mode and the O mode occupy different positions in the lattice and separate from each other half a period: (a) the slip field; (b) the discrete density distribution given by the difference of the slip between neighboring points.

in a model-independent way by using spectrum analysis. The spectrum $\widetilde{\Omega}(k)$ defined in the wave-vector space (k space) is given by Fourier transformation

$$\Omega(l) = \frac{D}{2\pi}\int_{-\frac{\pi}{D}}^{\frac{\pi}{D}} \widetilde{\Omega}(k)e^{ilkD}dk,$$

where D is distance between two neighboring atom chains parallel to the dislocation line. The $\widetilde{\Omega}(k)$ consists of the regular part $\widetilde{\Omega}_r(k)$ and singular part $\widetilde{\Omega}_s(k)$ [17–19]

$$\widetilde{\Omega}(k) = \widetilde{\Omega}_s(k) + \widetilde{\Omega}_r(k),$$

and in the leading term approximation,

$$\widetilde{\Omega}_r(k) = \omega^r(1-\cos kD), \quad \widetilde{\Omega}_s(k) = \omega^s\left|\sin\left(\frac{1}{2}kD\right)\right|,$$

where ω^r and ω^s are physics constants that need to be determined. From this phononlike spectrum, it is easy to obtain

$$\Omega_r(l) = \frac{D}{2\pi}\int_{-\frac{\pi}{D}}^{\frac{\pi}{D}} \widetilde{\Omega}_r(k)e^{ilkD}dk = \frac{\omega^r}{2}(2\delta_l - \delta_{l+1} - \delta_{l-1}),$$

$$\Omega_s(l) = \frac{D}{2\pi}\int_{-\frac{\pi}{D}}^{\frac{\pi}{D}} \widetilde{\Omega}_s(k)e^{ilkD}dk = -\frac{\omega^s}{2\pi}\frac{1}{l^2-\frac{1}{4}}.$$

Substituting $\Omega(l)$ in the leading term approximation into Eq. (1), one obtains (see the Appendix)

$$U_e = \frac{\omega^r}{4}\sum_{l=-\infty}^{\infty}\rho^2(l) - \frac{\omega^s}{4\pi}\sum_{l=-\infty}^{\infty}\sum_{l'=-\infty}^{\infty}\rho(l)\rho(l') \times \psi^{(0)}\left(|l-l'|+\frac{1}{2}\right) + \frac{Kb^2h}{4\pi}\ln\frac{R}{D}, \tag{2}$$

where $\rho(l) = S(l+1) - S(l)$ is the discrete dislocation density, $\psi^{(0)}(z)$ is the polygamma function, b is the Burgers vector, R measures the size of the crystal, K is the energy factor of a dislocation, and h is the period along the dislocation line. The last term is a constant resulting from selection of the potential energy zero point (the interaction energy approaches zero as far away in the distance). The elastic energy U_e is interpreted as the self-interaction energy of dislocation in a length of period h [20]. As shown in Fig. 2, the polygamma function is the substitute of the logarithmic function, which coincides with the logarithmic function as $|z| > 1$ and has no singularity at the origin $z = 0$. In the continuous approximation $x = lD$ ($D \to 0$),

$$\rho(l) = S(l+1) - S(l) \longrightarrow \frac{dS}{dx}D = \rho(x)D,$$

$$\sum_{l=-\infty}^{\infty} \longrightarrow \int_{-\infty}^{\infty}\frac{dx}{D}, \quad \psi^{(0)}\left(\frac{|x|}{D}+\frac{1}{2}\right) \longrightarrow \ln\frac{|x|}{D},$$

and the energy in unit length is

$$\frac{U_e}{h} = \frac{\omega^r D}{4h}\int_{-\infty}^{\infty}\rho^2(x)dx - \frac{\omega^s}{4\pi h}\int_{-\infty}^{\infty}\int_{-\infty}^{\infty}\rho(x)\rho(x') \times \ln\frac{|x-x'|}{D}dx\,dx' + \frac{Kb^2}{4\pi}\ln\frac{R}{D}. \tag{3}$$

The second term in Eq. (3) is just the energy functional given in the classical Peierls model [2]. Apparently, the classical Peierls model should be recovered as a continuous limit and thus the constant ω^s must be

$$\omega^s = \frac{K}{h} = \frac{K\tau}{D},$$

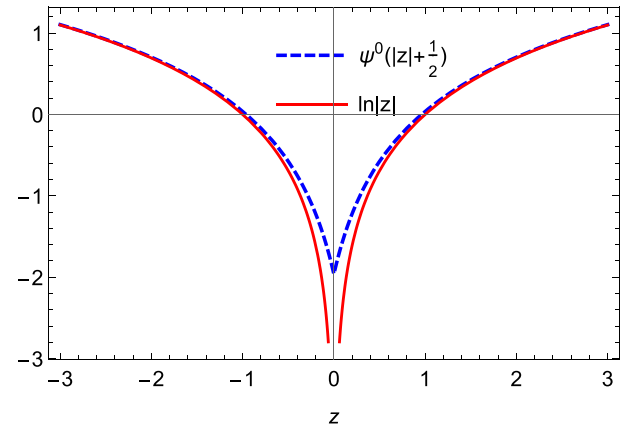

FIG. 2. Comparing the polygamma function with the logarithmic function.

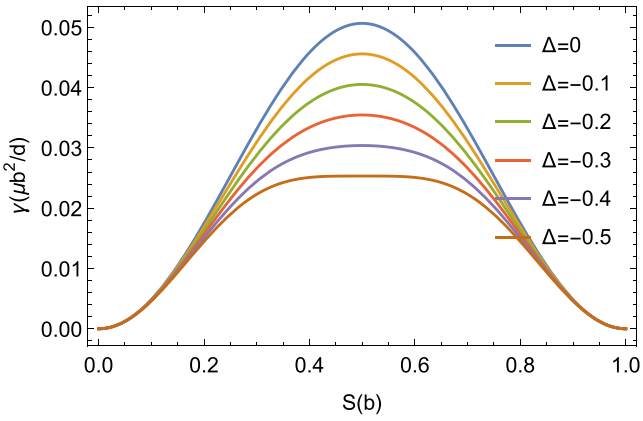

FIG. 3. γ surface for various values of the dimensionless parameter Δ.

where $\tau = hD$ is the area of the primitive cell of the slip plane. The first term in Eq. (3) represents the point-contact exclusive interaction that originates from lattice discreteness. The results of the exactly solvable model suggest that in the isotropic approximation the constant ω^r is $\mu\tau/D$ for the edge dislocation and $\mu\tau/2D$ for the screw dislocation, where μ is the shear modulus [21].

In the local approximation, the misfit energy is identified with the generalized stacking fault energy (γ surface) [7,22]

$$U_m = \sum_{l=-\infty}^{\infty} \gamma(S)\tau,$$
$$\gamma(S) = \frac{\mu b^2}{2\pi^2 d} \sin^2\frac{\pi S}{b}\left(1 + \Delta \sin^2\frac{\pi S}{b}\right), \tag{4}$$

where d is the spacing between the slip planes and Δ is a dimensionless parameter defined by the unstable stacking-fault energy γ_{us}

$$\gamma_{us} = \gamma\left(\frac{b}{2}\right) = \frac{\mu b^2}{2\pi^2 d}(1+\Delta). \tag{5}$$

As shown in Fig. 3, the γ surface is simply a single peak function for $\Delta > -0.5$.

The equilibrium dislocation structure is determined by the minimum energy principle

$$\frac{\delta U}{\delta S(l)} = 0, \quad U = U_e + U_m.$$

The explicit balance equation from the minimum energy principle is

$$-\frac{\omega^r}{4}[\rho(l) - \rho(l-1)] - \frac{\omega^s}{2\pi}\sum_{l'}\frac{\rho(l')}{l' - l + \frac{1}{2}} = -\frac{\partial\gamma}{\partial S}\tau. \tag{6}$$

However, if there is the resolved external stress σ, the balance is dominated by the Gibbs energy G

$$\frac{\delta G}{\delta S(l)} = 0, \quad G = U - \sum_{l=-\infty}^{\infty}\sigma S(l)\tau. \tag{7}$$

In practice, the stable structure and the response behavior to the external field can be more suitably studied by using the following time-dependent equation (Landau equation):

$$\Gamma\frac{\partial S}{\partial t} = -\frac{\delta G}{\delta S(l)}, \tag{8}$$

where Γ is an effective damping constant. In particular, when an arbitrary input function with the dislocation boundary condition is used as the initial condition, it will spontaneously relax to the stable equilibrium solution. In the following evaluation, the classical Peierls solution is employed as the initial input. After it has relaxed to the stable dislocation solution, the external stress is applied gradually to investigate how the dislocation responds. For the dissipation due to shear wave emission from the slip planes, the damping constant is $\Gamma = \mu\tau/(2c_t)$, where c_t is the shear wave velocity [23]. It is reasonable to measure the evolution time in the characteristic time scale b/c_t.

III. PEIERLS STRESS OSCILLATION

By using the theory presented above, the stable dislocation core structures and the Peierls stress are investigated numerically for the γ surface with various stacking fault energy. Because dislocations are highly localized modes, the slip can be neglected far away from the dislocation center. In practical numerical calculations, Eq. (8) is solved by truncating the lattice points number to be the finite one including 200 sites ($-100 \leqslant l \leqslant 100$). Surprisingly, it is found that the Peierls stress oscillates as the stacking fault energy decreases monotonically. As shown in Fig. 4, as a function of dimensionless parameter Δ that describes the magnitude of the stacking fault energy, the Peierls stress σ_p, defined by the critical external stress to make a dislocation move, clearly falls off in an oscillation way. The Peierls stress at oscillation nodes nearly vanishes ($\sigma_p \sim 10^{-6}\mu$). As a consequence, the dislocation can almost move freely. In addition, while the Peierls stress varies continuously with the dimensional parameter Δ, its derivative is not continuous at the nodes. Therefore, the nodes are singular points where something takes place in physics. A detailed examination reveals that nodes are the points at which transformation of the mode structures happens. For $0 \geqslant \Delta \geqslant -0.098$, the B mode has a lower energy $U_B < U_O$, and thus the B mode is stable. For $-0.098 \geqslant \Delta \geqslant -0.27$, the B mode loses stability and the O mode becomes a stable one. The node $\Delta = -0.098$ is the transition point. In the range $0 \geqslant \Delta \geqslant -0.5$, there are three transition points (nodes) distributed periodically (Fig. 4). Apparently, the energy difference between the B mode and O mode vanishes at the transition points, $U_O - U_B = 0$.

While a continuous mode can locate at any point, the possible positions of the B mode or the O mode are a series of discrete points that are aligned periodically. It can be observed that the B mode and the O mode are distinct from each other not only in the structure, but also in the positions defined by the symmetric center. Once the B mode is transformed into the O mode, or otherwise, it moves forward (or backward) a step that equals half a period. Therefore, mode movement can be realized by sequent transformations:

$$B \to O \to B \to O \to B \to O \to B \cdots.$$

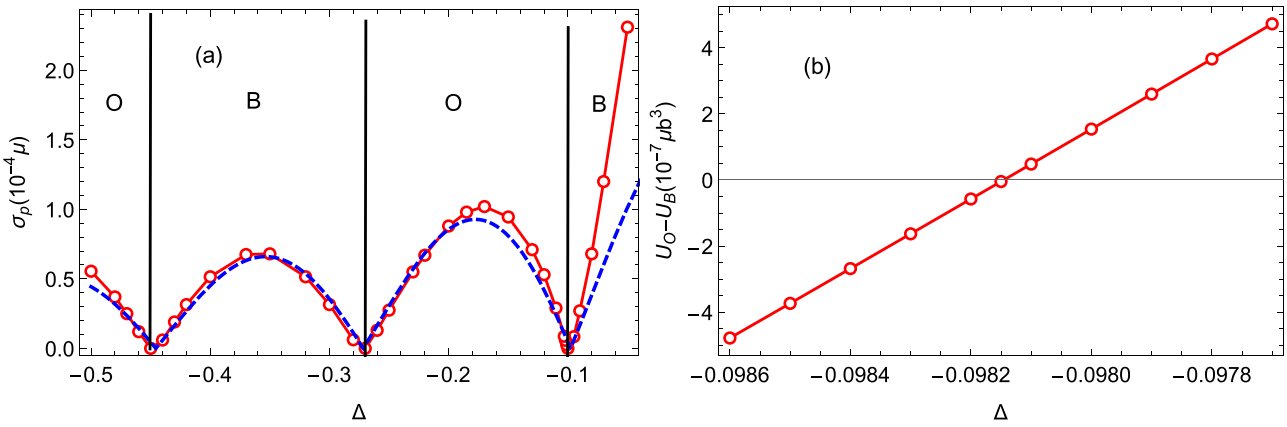

FIG. 4. (a) Peierls stress oscillation of the pure edge dislocation in the cubic lattice with the γ surface given by Eq. (4); the dashed line is given by the fit Eq. (10). (b) The energy difference between the B mode and the O mode near the first node. The Poisson ratio $\nu \approx 1/3$ is used in calculation. The oscillation originates from stability transformation between the B mode and the O mode.

The transformation from a stable mode to a unstable mode needs to overcome the energy barrier. The energy difference in a unit length between the O mode and the B mode is defined as the PN barrier of a dislocation:

$$E_p = \frac{|U_O - U_B|}{h}.$$

The higher the PN barrier is, the more difficult to transform, and thus the more robust the stable mode is. Because the energy of the B mode (or the O mode) should be a smooth function of Δ, near the transition point Δ_c, the PN barrier must vary in the form $E_p \propto |\Delta - \Delta_c|$. For the first transition point of the edge dislocation, the data from numerical calculation suggest $E_p = 1.0567 \times |\Delta + 0.098146| \times 10^{-3}\ \mu b^2$.

The Peierls stress is mainly determined by the PN barrier. In the classical PN model, the Peierls stress is proportional to the barrier height in the leading term approximation

$$\sigma_p = \frac{\pi E_p}{bD} = 3.32 \times |\Delta + 0.098146| \times 10^{-3}\ \mu. \quad (9)$$

On the other hand, as shown in Fig. 4, the global behavior of the Peierls stress of the edge dislocation can be well fitted by

$$\sigma_p = \left|\frac{0.4\ \sin 5.75\pi(\Delta - 0.25)}{\Delta - 0.25}\right| \times 10^{-4}\ \mu. \quad (10)$$

Near the critical point $\Delta_c = -0.098146$, this expression becomes $\sigma_p = (0.0006 + 2.07 \times |\Delta + 0.098146|) \times 10^{-3}\ \mu$. The accuracy predicted from the leading term approximation Eq. (9) is acceptable when the first term in brackets is negligible. Theoretically, the Peierls stress around a transition point can be expanded into the power series

$$\sigma_p = \sigma_p^{(0)} + \sigma_p^{(1)}|\Delta - \Delta_c|. \quad (11)$$

If $\sigma_p^{(0)} = 0$, the Peierls stress is proportional to the PN barrier, and thus it is exactly equal to zero at the transition points. However, present numerical evaluations indicate that $\sigma_p^{(0)} \sim 10^{-6}\ \mu$ and $\sigma_p^{(1)} \sim 10^{-3}\ \mu$ for the edge dislocation. Therefore, although the PN barrier disappears at the transition points, the Peierls stress does not completely vanish. There exists extra contribution to the lattice friction beyond the PN barrier in the fully discrete Peierls model. The origination and physical mechanism of the extra lattice friction remains elusive.

In the 1990s, Speight and Ward, using the Bogomol'nyi argument, showed that for specially discretized nonlinear models there may exist static kink solutions occupying any position relative to the lattice [24,25]. Consequently, kinks of the models experience no PN barrier and can be quasistatically moved through the lattice without being pinned. Recently, a variety of models free of the PN barrier are proposed and studied [26–29]. The fully discrete Peierls model can also be viewed as a model free of the PN barrier. However, it is more rational to explain phenomena revealed above by activation of the intrinsic freedom of dislocation structures.

IV. SCREW DISLOCATIONS IN FACE CENTERED CUBIC (FCC) LATTICE

Dislocations in real materials frequently involve both the edge and screw components. In the isotropic approximation, the energy functional is given by

$$U = \frac{\mu\tau}{4D}\sum_{l=-\infty}^{\infty}\left[\rho_e^2(l) + \frac{1}{2}\rho_s^2(l)\right] - \frac{\mu\tau}{4\pi D}\sum_{l=-\infty}^{\infty}\sum_{l'=-\infty}^{\infty}\left[\frac{\rho_e(l)\rho_e(l')}{1-\nu} + \rho_s(l)\rho_s(l')\right] \times \psi^{(0)}\left(|l-l'| + \frac{1}{2}\right) + \sum_{l=-\infty}^{\infty}\gamma(S_e, S_s)\tau + \frac{Kb^2h}{4\pi}\ln\frac{R}{D}, \quad (12)$$

where subscripts e and s are used to label the edge and screw parts. As an application, the screw dislocation lying along the $\langle 110\rangle$ direction in the fcc lattice is studied with the γ surface of the (111) plane [30]

$$\gamma(S_e, S_s) = \frac{\mu b^2}{4\pi^2 d}\left[1 - \cos\frac{2\pi S_s}{b}\cos\frac{2\pi S_e}{\sqrt{3}b} + \sin^2\frac{2\pi S_e}{\sqrt{3}b} + \Delta\left(\cos\frac{2\pi S_e}{\sqrt{3}b} - \cos\frac{2\pi S_s}{b}\right)\sin\frac{2\pi S_e}{\sqrt{3}b}\right]. \quad (13)$$

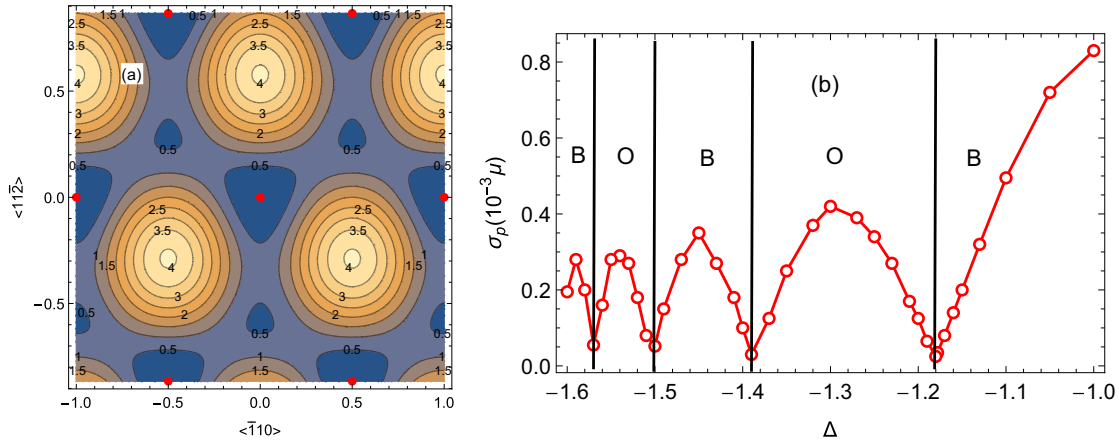

FIG. 5. (a) γ surface given by Eq. (13) with $\Delta = -1.4$, where energy and length are measured respectively in the units of $\mu b^2/(4\pi^2 d)$ and b. (b) The Peierls stress oscillation for the $\langle\bar{1}10\rangle$ screw dislocation in the fcc lattice.

In Fig. 5, the γ surface given by Eq. (13) with $\Delta = -1.4$ and the Peierls stress versus dimensionless parameter Δ are plotted. In Fig. 6 and Fig. 7, the slip field and the density distribution are shown for typical values of the dimensionless parameter Δ. Similarly, the Peierls stress oscillation and the mode transformation appear as the Δ changes monotonically. However, the oscillation period decreases gradually, and the residual stress $\sigma_p^{(0)}$ increases obviously compared with the edge dislocation discussed above. Because the dimensionless parameter Δ actually represents the stacking fault energy of the fcc lattice, $\gamma_s = 9\mu b^2(1 + \Delta/\sqrt{3})/(16\pi^2 d)$, the core type of dislocation structure may be controlled by changing the stacking fault energy γ_s [16,31]. In Table I, values of the dimensionless parameter Δ are listed for some typical metals with fcc lattice structure.

V. SUMMARY

In summary, the stability of discrete modes and relevant implication are studied in the framework of the fully discrete Peierls model. The conventional continuous mode splits into the B mode and the O mode, which have little difference in continuous envelope, but have distinct structures on the atom scale. The mode with lower energy is stable. Therefore, on the atomic scale, dislocations in materials may display two different structures characterized theoretically by the B mode and the O mode. It is necessary to carefully examine the dislocation core in experiments and numerical simulations to determine which type it is. Transformation between the B mode and the O mode implies activation of a freedom of dislocation structure [13]. Here, the mode stability and transformation have been specifically investigated as a function of the stacking fault energy parametrized by a dimensionless constant Δ. A sequential transformation series is clearly revealed as Δ changes in a physical range. Peierls stress oscillation originates from the dislocation structure transformation. It is predicted that the lattice resistance is drastically reduced at the transition points due to Peierls barrier vanishing. In general, the dislocation core structure is determined mainly by both the stacking fault energy and the elastic constants of bulk material. It is well known that the stacking fault energy and the elastic constants are strongly dependent of temperature and pressure, and other factors such as alloying and deformation [15,16,31,32]. Therefore, the type of dislocation structure may be tuned artificially and material plasticity may be substantially altered as approaching the transition points.

ACKNOWLEDGMENT

This work was supported by the National Natural Science Foundation of China (NNSFC) (Grants No. 11874093 and No. 12147102).

APPENDIX

In this Appendix, the energy functional Eq. (2) is derived in detail. Due to the discrete displacement symmetry, the elastic energy in the harmonic approximation of the interaction can be generally expressed as

$$U_e = \frac{1}{2}\sum_l \sum_{l'} \Omega(l - l')S(l)S(l'). \tag{A1}$$

TABLE I. Dimensional parameter Δ for typical fcc metals [30].

Metal	Cu	Ag	Au	Al	Ni	Rh	Pd	Pt	Pb
Δ	−1.63	−1.67	−1.61	−1.35	−1.66	−1.54	−1.45	−1.10	−1.37

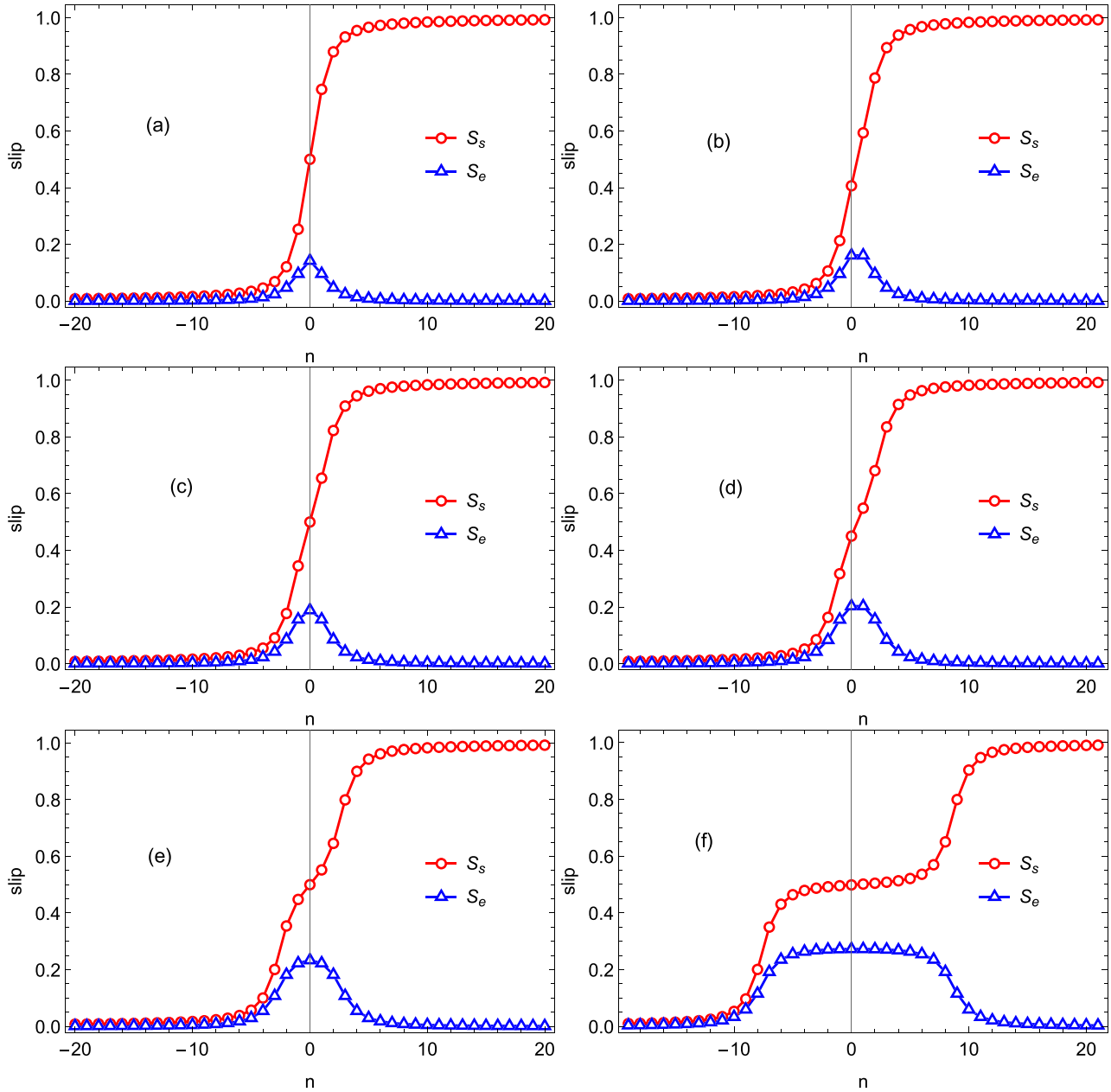

FIG. 6. Screw component S_s and the edge component S_e of the slip field of the screw dislocation in the fcc lattice: (a) $\Delta = -1.1$, (b) $\Delta = -1.3$, (c) $\Delta = -1.4$, (d) $\Delta = -1.5$, (e) $\Delta = -1.6$, and (f) $\Delta = -1.7$, where the slip is measured in units of the Burgers vector b and the Poisson ratio $\nu = 1/3$ is taken in evaluation.

Hereafter, the summation index always runs over all integers if it is not specified explicitly. In the leading terms approximation

$$\Omega(l) = \Omega_s(l) + \Omega_r(l),$$
$$\Omega_s(l) = -\frac{\omega^s}{2\pi}\frac{1}{l^2 - \frac{1}{4}},$$
$$\Omega_r(l) = \frac{\omega^r}{2}(2\delta_l - \delta_{l+1} - \delta_{l-1}).$$

Thus the energy is a sum of two terms

$$U_e = U_e^r + U_e^s,$$
$$U_e^r = \frac{1}{2}\sum_l \sum_{l'} \Omega_r(l - l')S(l)S(l'),$$
$$U_e^s = \frac{1}{2}\sum_l \sum_{l'} \Omega_s(l - l')S(l)S(l').$$

Before proceeding to the Eq. (2) derivation, it is helpful to develop the difference and summation calculus that is similar to the differential and integral calculus. Let us introduce the

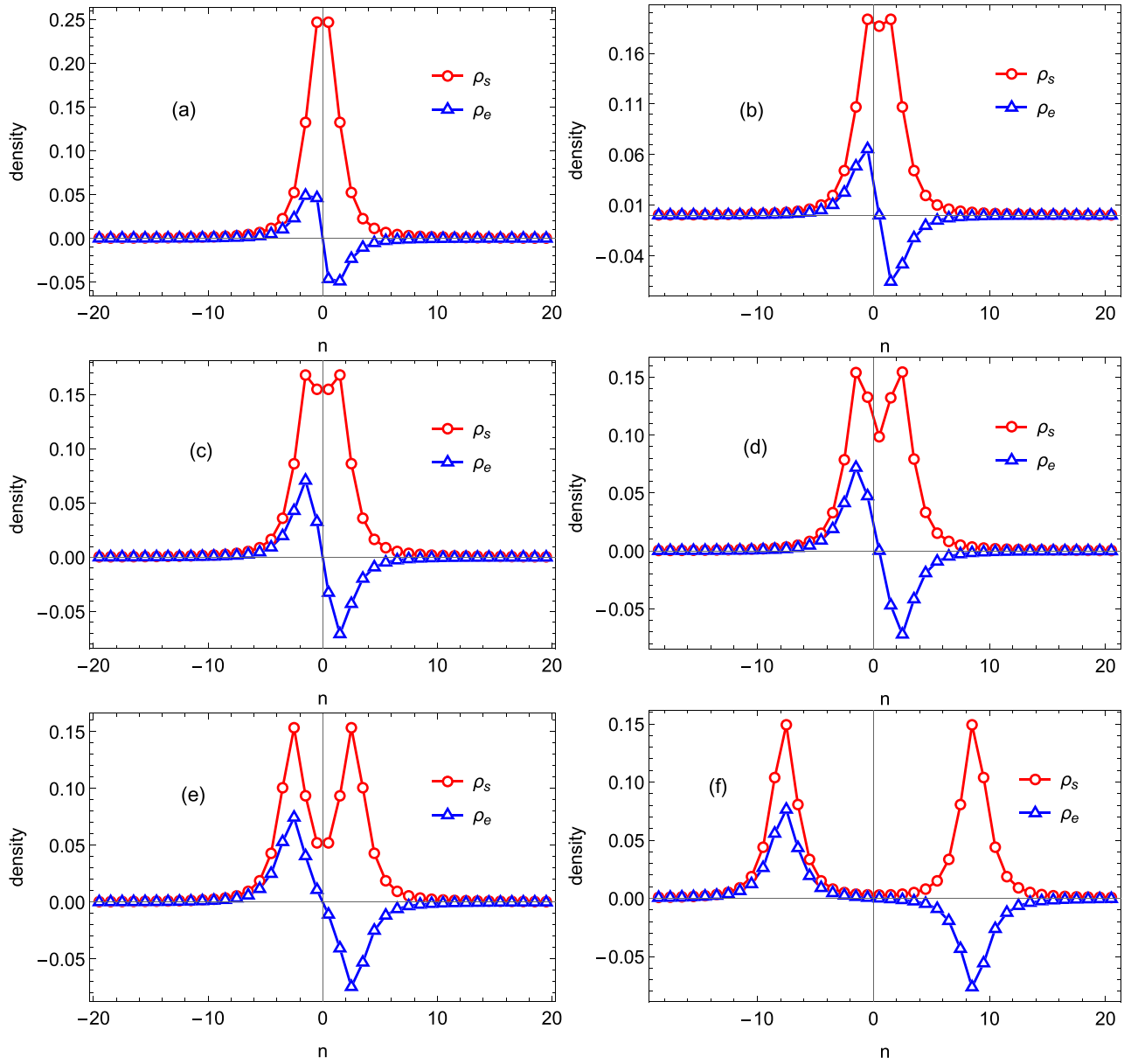

FIG. 7. Dislocation density distribution given by the discrete gradient of the slip field: (a) $\Delta = -1.1$, compact O mode, (b) $\Delta = -1.3$, slightly dissociated B mode, (c) $\Delta = -1.4$, dissociated O mode, (d) $\Delta = -1.5$, dissociated B mode, (e) $\Delta = -1.6$, dissociated O mode, and (f) $\Delta = -1.7$, highly dissociated B mode.

forward difference operator ∇ and the backward difference operator $\bar{\nabla}$

$$\nabla S(l) = S(l+1) - S(l), \quad \bar{\nabla} S(l) = S(l) - S(l-1).$$

The density is defined as the forward difference of the slip

$$\rho(l) = \nabla S(l).$$

Obviously,

$$\bar{\nabla} S(l) = \rho(l-1).$$

For the difference operation of the product, there are identities similar to the formula well known in the differential calculus

$$\begin{aligned}\nabla(S\rho) &= S(l+1)\rho(l+1) - S(l)\rho(l) \\ &= S(l+1)\rho(l+1) - S(l)\rho(l+1) + S(l)\rho(l+1) \\ &\quad - S(l)\rho(l) \\ &= \rho(l+1)\nabla S + S(l)\nabla\rho = S(l+1)\nabla\rho + \rho(l)\nabla S\end{aligned} \tag{A2}$$

and

$$\begin{aligned}\bar{\nabla}(S\rho) &= S(l)\rho(l) - S(l-1)\rho(l-1) \\ &= \rho(l)\bar{\nabla}S + S(l-1)\bar{\nabla}\rho = S(l)\bar{\nabla}\rho + \rho(l-1)\bar{\nabla}S,\end{aligned} \tag{A3}$$

where the last steps come from exchange invariance between S and ρ. In analogy to the Newton-Leibniz integral formula, there is summation identity

$$\sum_{l=l_0}^{l=l_1} \nabla S(l) = S(l_0+1) - S(l_0) + S(l_0+2) - S(l_0+1) + \cdots + S(l_1+1) - S(l_1) = S(l_1+1) - S(l_0),$$

where the intermediate terms cancel each other and only two boundary values remain. In analogy,

$$\sum_{l=l_0}^{l=l_1} \bar{\nabla} S(l) = S(l_1) - S(l_0-1).$$

In physics, variational derivative of the energy is the force

$$f(l) = -\frac{\delta U}{\delta S(l)} = -\sum_{l'} \Omega(l-l')S(l').$$

Obviously, energies U_e^r and U_e^s can be written as

$$\begin{aligned} U_e^r &= -\frac{1}{2}\sum_l f_r(l)S(l), \\ f_r(l) &= -\frac{\delta U_e^r}{\delta S(l)} = -\sum_{l'} \Omega_r(l-l')S(l'), \\ U_e^s &= -\frac{1}{2}\sum_l f_s(l)S(l), \\ f_s(l) &= -\frac{\delta U_e^s}{\delta S(l)} = -\sum_{l'} \Omega_s(l-l')S(l'). \end{aligned} \tag{A4}$$

For the $\Omega_r(l)$, the related force is

$$\begin{aligned} f_r(l) &= -\sum_{l'} \Omega_r(l-l')S(l') = -\sum_{l'} \frac{\omega^r}{2}(2\delta_{l-l'} - \delta_{l-l'+1} - \delta_{l-l'-1})S(l') \\ &= -\frac{\omega^r}{2}[2S(l) - S(l+1) - S(l-1)] = \frac{\omega^r}{2}\bar{\nabla}\nabla S(l) = \frac{\omega^r}{2}\bar{\nabla}\rho(l) \end{aligned} \tag{A5}$$

and the energy is

$$\begin{aligned} U_e^r(l) &= -\frac{1}{2}\sum_l f_r(l)S(l) = -\frac{\omega^r}{4}\sum_l S(l)\bar{\nabla}\rho(l) \\ &= -\frac{\omega^r}{4}\sum_l [\bar{\nabla}(S\rho) - \rho(l-1)\bar{\nabla}S(l)] = \frac{\omega^r}{4}\sum_l \rho^2(l), \end{aligned} \tag{A6}$$

where the condition $\rho(\pm\infty) = 0$ has been used in the last equality.

For the $\Omega_s(l)$, the force is

$$\begin{aligned} f_s(l) &= -\sum_{l'} \Omega_s(l-l')S(l') = \frac{\omega^s}{2\pi}\sum_{l'} \frac{S(l')}{(l-l')^2 - \frac{1}{4}} \\ &= \frac{\omega^s}{2\pi}\sum_{l'}\left[\frac{S(l')}{l-l'-\frac{1}{2}} - \frac{S(l')}{l-l'+\frac{1}{2}}\right] \\ &= \frac{\omega^s}{2\pi}\sum_{l'} \frac{S(l') - S(l'+1)}{l-l'-\frac{1}{2}} = -\frac{\omega^s}{2\pi}\sum_{l'} \frac{\rho(l')}{l-l'-\frac{1}{2}} \end{aligned} \tag{A7}$$

and the energy is

$$\begin{aligned} U_e^s(l) &= -\frac{1}{2}\sum_l f_s(l)S(l) = \frac{\omega^s}{4\pi}\sum_l\sum_{l'} \frac{\rho(l')S(l)}{l-l'-\frac{1}{2}} \\ &= \frac{\omega^s}{4\pi}\sum_{l'} \rho(l')\sum_l \frac{S(l)}{l-l'-\frac{1}{2}}. \end{aligned} \tag{A8}$$

Introducing function φ by the following equation:

$$\nabla\varphi\left(l-l'-\frac{1}{2}\right) = \varphi\left(l+1-l'-\frac{1}{2}\right) - \varphi\left(l-l'-\frac{1}{2}\right) = \frac{1}{l-l'-\frac{1}{2}},$$

from Eq. (A2) the last summation in Eq. (A8) can be changed into

$$\sum_l \frac{S(l)}{l-l'-\frac{1}{2}} = \sum_l S(l)\nabla\varphi\left(l-l'-\frac{1}{2}\right) = \sum_l \left[\nabla(S\varphi) - \varphi\left(l+1-l'-\frac{1}{2}\right)\nabla S(l)\right]$$
$$= \sum_l \nabla(S\varphi) - \sum_l \varphi\left(l-l'+\frac{1}{2}\right)\rho(l). \tag{A9}$$

The function $\varphi(l-l'+\frac{1}{2})$ can be obtained exactly. It is given by

$$\varphi\left(l-l'-\frac{1}{2}\right) = \psi^0\left(|l-l'|-\frac{1}{2}\right) + \varphi_0, \tag{A10}$$

where φ_0 is an arbitrary constant. $\psi^0(z)$ is the polygamma function defined by the Gamma function $\Gamma(z)$

$$\psi^0(z) = \frac{1}{\Gamma(z)}\frac{d\Gamma(z)}{dz}, \quad \psi^0(z+1) - \psi^0(z) = \frac{1}{z}.$$

The function φ actually describes the interaction energy between two dislocations $\rho(l)$ and $\rho(l')$. It is physically rational to choose the constant $\varphi_0 = -\psi^0(N\to\infty)$ to make the interaction energy vanish when two dislocations are far apart:

$$\varphi\left(l-l'-\frac{1}{2}\right) = \psi^0\left(|l-l'|-\frac{1}{2}\right) - \psi^0(N), \quad N\to\infty.$$

As a result of selection of potential energy zero point, the first term of the last expression in Eq. (A9) is zero. The energy U_e^s now is

$$U_e^s(l) = -\frac{\omega^s}{4\pi}\sum_l\sum_{l'}\varphi\left(l-l'+\frac{1}{2}\right)\rho(l')\rho(l')$$
$$= -\frac{\omega^s}{4\pi}\sum_l\sum_{l'}\psi^0\left(l-l'+\frac{1}{2}\right)\rho(l')\rho(l') + \frac{\omega^s}{4\pi}\sum_l\sum_{l'}\psi^0(N)\rho(l)\rho(l')$$
$$= -\frac{\omega^s}{4\pi}\sum_l\sum_{l'}\psi^0\left(l-l'+\frac{1}{2}\right)\rho(l')\rho(l') + \frac{\omega^s b^2}{4\pi}\ln\frac{R}{D}, \tag{A11}$$

where R is a macroscopic length and D is the period in direction perpendicular to the dislocation line, and

$$\sum_l \rho(l) = b, \quad \psi^0(N) = \ln N = \ln\frac{R}{D}, \quad N\to\infty,$$

are used.

In summary,

$$U_e = \frac{\omega^r}{4}\sum_{l=-\infty}^{\infty}\rho^2(l) - \frac{\omega^s}{4\pi}\sum_{l=-\infty}^{\infty}\sum_{l'=-\infty}^{\infty}\rho(l)\rho(l')\psi^{(0)}\left(|l-l'|+\frac{1}{2}\right) + \frac{\omega^s b^2}{4\pi}\ln\frac{R}{D}. \tag{A12}$$

This elastic energy U_e is the self-interaction energy of dislocation in a length of period h. In the continuous approximation, the classical PN model should be recovered, and thus the constant ω^s must be

$$\omega^s = \frac{K\tau}{D},$$

where $\tau = hD$ is the area of the primitive cell of a slip plane. Because the dislocation radius r_0 (dislocation width) introduced in the continuum elasticity theory approximately equals the lattice characteristic length D, $r_0 \sim D$, the last term is roughly the same as the dislocation energy given in the continuum elasticity theory

$$U_e^0 = \frac{\omega^s b^2}{4\pi}\ln\frac{R}{D} = \frac{Kb^2 h}{4\pi}\ln\frac{R}{D}.$$

The first two terms can be referred to as the dislocation core energy

$$U_e^c = \frac{\omega^r}{4}\sum_{l=-\infty}^{\infty}\rho^2(l) - \frac{\omega^s}{4\pi}\sum_{l=-\infty}^{\infty}\sum_{l'=-\infty}^{\infty}\rho(l)\rho(l')$$
$$\times\,\psi^{(0)}\left(|l-l'|+\frac{1}{2}\right). \tag{A13}$$

[1] J. P. Hirth and J. Lothe, *Theory of Dislocations*, 2nd ed. (Wiley, New York, 1982).

[2] R. Peierls, The size of a dislocation, Proc. Phys. Soc. **52**, 34 (1940).

[3] M. S. Duesbery and G. Y. Richardson, The dislocation core in crystalline materials, Solid State Mater. Sci. **17**, 1 (1991).
[4] W. Cai, V. V. Bulatov, J. Chang, J. Li, and S. Yip, Dislocation core effects on mobility, Dislocat. Solids **12**, 1 (2005).
[5] D. Rodney, L. Ventelon, E. Clouet, L. Pizzagalli, and F. Willaime, Ab initio modeling of dislocation core properties in metals and semiconductors, Acta Mater. **124**, 633 (2017).
[6] J. Bennetto, R. W. Nunes, and D. Vanderbilt, Period-Doubled Structure for the 90° Partial Dislocation in Silicon, Phys. Rev. Lett. **79**, 245 (1997).
[7] J. W. Chrisrian and V. Vítek, Dislocations and stacking faults, Rep. Prog. Phys. **33**, 307 (1970).
[8] V. Vitek, Theory of the core structures of dislocations in bcc metals, Cryst. Lattice Defects **5**, 1 (1974).
[9] B. Joós, Q. Ren, and M. S. Duesbery, Peierls-Nabarro model of dislocations in silicon with generalized stacking-fault restoring forces, Phys. Rev. B **50**, 5890 (1994).
[10] V. V. Bulatov and E. Kaxiras, Semidiscrete Variational Peierls Framework for Dislocation Core Properties, Phys. Rev. Lett. **78**, 4221 (1997).
[11] G. Lu, N. Kioussis, V. V. Bulatov, and E. Kaxiras, Generalized-stacking-fault energy surface and dislocation properties of aluminum, Phys. Rev. B **62**, 3099 (2000).
[12] G. Schoeck, The Peierls model: Progress and limitations, Mater. Sci. Eng. A **400-401**, 7 (2005).
[13] Z. Wang, M. Saito, K. P. McKenna, and Y. Ikuhara, Polymorphism of dislocation core structures at the atomic scale, Nat. Commun. **5**, 3239 (2014).
[14] S. Wang, L. Huang, and R. Wang, The 90° partial dislocation in semiconductor silicon: An investigation from the lattice P-N theory and the first principle calculation, Acta Mater. **109**, 187 (2016).
[15] H. Xiang, R. Wang, and S. Wang, Core structure and thermal transformation of the $1/2 < 110 > (111)$ screw dislocation in aluminum, J. Appl. Phys. **127**, 125106 (2020).
[16] Z. Pei, B. Dutta, F. Körmann, and M. Chen, Hidden Effects of Negative Stacking Fault Energies in Complex Concentrated Alloys, Phys. Rev. Lett. **126**, 255502 (2021).
[17] S. Wang, Lattice theory for structure of dislocations in a two-dimensional triangular crystal, Phys. Rev. B **65**, 094111 (2002).
[18] S. Wang, Dislocation equation from the lattice dynamics, J. Phys. A: Math. Theor. **41**, 015005 (2008).
[19] S. Wang, An improvement of the Peierls equation by taking into account the lattice effects, Chin. Phys. **14**, 2575 (2005).
[20] J. D. Eshelby, The continuum theory of lattice defects, Solid State Phys. **3**, 79 (1956).
[21] S. Wang, Boundary equation from a lattice model and modification of the Peierls equation, Philos. Mag. **102**, 1 (2022).
[22] W. Shao-Feng, W. Xiao-Zhi, and W. Yin-Feng, Variational principle for the dislocation equation in lattice theory, Phys. Scr. **76**, 593 (2007).
[23] Y.-P. Pellegrini, Dynamic Peierls-Nabarro equations for elastically isotropic crystals, Phys. Rev. B **81**, 024101 (2010).
[24] E. B. Bogomol'nyi, The stability of classical solutions, Sov. J. Nucl. Phys. **24**, 449 (1976).
[25] J. M. Speight and R. S. Ward, Kink dynamics in a novel discrete sine-gordon system, Nonlinearity **7**, 475 (1994).
[26] S. V. Dmitriev, P. G. Kevrekidis, N. Yoshikawa, and D. J. Frantzeskakis, Exact static solutions for discrete ϕ^4 models free of the Peierls-Nabarro barrier: Discretized first-integral approach, Phys. Rev. E **74**, 046609 (2006).
[27] B. Prinari, M. J. Ablowitz, and A. D. Trubatch, *Discrete and Continuous Nonlinear Schrödinger Systems* (Cambridge University Press, Cambridge, England, 2004).
[28] Z. Xu, Y. V. Kartashov, and L. Torner, Soliton Mobility in Nonlocal Optical Lattices, Phys. Rev. Lett. **95**, 113901 (2005).
[29] H. Susanto, P. G. Kevrekidis, R. Carretero-González, B. A. Malomed, and D. J. Frantzeskakis, Mobility of Discrete Solitons in Quadratically Nonlinear Media, Phys. Rev. Lett. **99**, 214103 (2007).
[30] X. Wu, R. Wang, S. Wang, and Q. Wei, *Ab initio* calculations of generalized-stacking-fault energy surfaces and surface energies for FCC metals, Appl. Surf. Sci. **256**, 6345 (2010).
[31] X. Zhang, B. Grabowski, F. Körmann, A. V. Ruban, Y. Gong, R. C. Reed, T. Hickel, and J. Neugebauer, Temperature dependence of the stacking-fault Gibbs energy for Al, Cu, and Ni, Phys. Rev. B **98**, 224106 (2018).
[32] W. Z. Han, G. M. Cheng, S. X. Li, S. D. Wu, and Z. F. Zhang, Deformation Induced Microtwins and Stacking Faults in Aluminum Single Crystal, Phys. Rev. Lett. **101**, 115505 (2008).